

# Study of Abrasive Wear of Al-Zn-Mg Alloy by Taguchi Method

Surbhi Bisen<sup>1</sup>, Tejas Umale<sup>2</sup>, Yogesh Mahajan<sup>1</sup>, D. R. Peshwe<sup>1</sup>

<sup>1</sup>Department of Metallurgical and Materials Engineering, Visvesvaraya National Institute of Technology, Nagpur, Maharashtra, India

## Abstract

The present study reports the abrasive wear behaviour of Al-Zn-Mg alloy in peak aged condition. The wear test was conducted on pin-on-disc machine. The hardness was reported and micrographs were also taken. Experimental design generated through Taguchi's technique was used to conduct experiments based on  $L_9$  orthogonal array and signal-to-noise ratio, the smaller-the better, was selected. ANOVA was employed to investigate the influence of wear parameters; applied load, sliding velocity, sliding time and abrasive particle size on specimens. The correlation was obtained by multiple general regression model. Finally, confirmation test was done to make a comparison between the experimental results foreseen from the mentioned correlation. SEM images of wear tracks and debris depicting mild, medium and severe wear were taken.

## 1. Introduction

Aluminium (Al) is the second-most plentiful element on earth and it became an economic competitor in the engineering applications as early as the end of the 19th century. Al and Al alloys have many outstanding attributes that lead to a wide range of applications, including good corrosion and oxidation resistance, high electrical and thermal conductivities, low density, high reflectivity, high ductility and reasonably high strength, and relatively low cost. Al is a lightweight material with a density of  $2.7 \text{ g/cm}^3$ . Pure Al and its alloys have the face-centered cubic (fcc) structure, which is stable up to its melting point at  $657^\circ\text{C}$  ( $1215^\circ\text{F}$ ). As the fcc structure contains multiple slip

planes, this crystalline structure greatly contributes to the excellent formability of Al alloys. Al alloys display a good combination of strength and ductility. Al alloys are among the easiest of all metals to form and machine. The precipitation hardening alloys can be formed in a relatively soft state and then heat treated to much higher strength levels after forming operations are complete. In addition, Al and its alloys are non-toxic and among the easiest to recycle of any of the structural materials [4-6].

Al alloys are normally classified into one of three groups: wrought non-heat treatable alloys, wrought heat treatable alloys, and casting alloys. Wrought non-heat-treatable alloys cannot be strengthened by precipitation hardening; they are hardened primarily by cold working. Casting alloys include both non-heat-treatable and heat treatable alloys. Wrought heat treatable alloys can be precipitation hardened to its peak strength by proper ageing conditions. These alloys include the 2xxx series (Al-Cu and Al-Cu-Mg), the 6xxx series (Al-Mg-Si), the 7xxx series (Al-Zn-Mg and Al-Zn-Mg-Cu), and the Al-Li alloys of the 8xxx alloy series. Among the above series, 7xxx series Al alloys are very strong "heat treatable" alloys; they can be strengthened through heat treatment (precipitation hardening) based on the combination of zinc (mostly between 4–6 wt %) and magnesium (range 1–3 wt %). The coherent and semicoherent precipitates are typically of the type  $\text{Mg}_x\text{Zn}_y$  [4-6].

Important critical applications of these alloys are based on their superior strength in peak aged condition, for example, in aerospace, space exploration, military and nuclear applications. These alloys find wide application in automobile engines components because of high strength to weight ratio. They are also used in applications such as structural components for tooling

plates; and also in structural parts in building applications. These are mostly used in peak aged conditions (T6 temper) to gain the advantage of high specific strength. Thus it becomes all the more vital to study the tribological characteristics of Al-Zn-Mg alloys in peak aged condition. Abrasive wear is supposed to occur on a soft metal surface abraded by hard and sharp abrasive particles [1]. It has been estimated that 50% of all wear problems in industry are due to abrasion [2-3], and hence more attention is required to study the abrasive wear behavior of such critical alloys.

## 2. Wear

Wear is a progressive loss of material from the surface of a solid, brought about by mechanical causes, i.e., by contact and relative motion of a solid, fluid or gaseous counter body. Signs of wear are small detached wear particles, material removal from one friction body to the other, and material and shape changes of the tribologically loaded material zone of one or both friction partners. Abrasive wear occurs whenever a solid object is loaded against particles of a material that have equal or greater hardness [7].

## 3. Taguchi Technique

The Taguchi method drastically reduces the number of experiments that are required to model response function compared with full factorial design of experiments. The method has been used widely in engineering analysis to optimise performance characteristics through design parameter settings. The three step procedure for experimental design includes: (1) finding the total degree of freedom (DOF) (2) selecting a standard orthogonal array such that the number of runs in the orthogonal design  $\geq$  total DOF and the selected orthogonal array should be able to accommodate the factor level combinations in the experiment (3) assigning factors appropriate columns. Some of the many advantages of this technique include (1) designs orthogonal arrays to balance process parameters and minimise test runs (2) employs signal-to-noise (S/N) ratio to analyse experiment data, and conclude more information. Taguchi suggests the use of the S/N ratio for determining quality characteristics implemented in engineering design problems. (3) estimates individual parameter contribution [8-9].

## 4. Objective of the study

To study the abrasive wear behaviour of Al-Zn-Mg alloy in peak aged condition based on Taguchi method using pin-on-disc type testing machine. Further, the analysis of variance is employed to investigate the testing characteristics of this alloy.

## 5. Experimental Details

Cylindrical pieces of dimensions, 10mm diameter and 25mm length, were prepared for wear testing from forged bar of Al-Zn-Mg alloy. These cylindrical specimens were cut using the Electric Discharge Machine. The chemical analysis of the forged bar is indicated in Table 1. The experimental density of this alloy is 2.83 g/cc. The specimens were soaked at 475 °C in furnace for an hour and then quenched in water. Hardness was measured to be around 92.3 HV under load of 5 kgf in solutionized condition. The pieces were then soaked at 120°C for one day in air circulating oven. Hardness in T6 condition was measured to be around 180.4 HV under load of 5 kgf.

**Table 1. Nominal chemical composition of the Al-Zn-Mg alloy**

Element	Content (at. %)
Al	89.50
Zn	06.10
Mg	02.50

## 6. Wear Test

A pin-on-disc machine was used to evaluate wear characteristics of specimens under dry sliding wear conditions. The wear tests were performed at room temperature. The emery paper (SiC abrasive paper) was fixed to 8mm thick and 160 mm diameter steel disc to serve as abrasive medium. The specimens were cleaned with acetone and the initial weight of each specimen was noted using a digital electronic balance. The pin was then mounted on a steel holder in the wear machine so that it was held firmly perpendicular to that of the flat surface of the rotating counter disc when tested. The radius of the sliding track was 40mm. The samples were loaded against the abrasive medium by a cantilever mechanism. The parameters were set according to experimental requirement. As soon as the time was over, machine stopped automatically and the specimen was taken out. The debris was carefully collected and preserved for further studies. At the end of each test, the pin was weighed again after cleaning

the worn out surface of the specimen with ethyl alcohol and then by jet air cleaning technique. The difference between the initial and the final weights was taken as a measure of slide mass loss. The wear rate  $W$  ( $m^2/N$ ) was calculated using the following equation:

$$W = \frac{\Delta m}{\rho \cdot t \cdot \omega \cdot 2\pi r \cdot F} \quad \dots \text{Equation (1)}$$

where,  $\Delta m$  is the mass loss on pin samples (g),  $\rho$  is the density of the test sample ( $g/m^3$ ),  $t$  is the test duration (minutes),  $\omega$  is sliding velocity (rpm),  $r$  is the radius of the sliding track of pin (m),  $F$  is the average normal load (N).

A standard Taguchi experimental plan with  $L_9$  ( $3^4$ ) array was chosen for the statistical analysis as indicated in Table 2. The selection of the orthogonal array is based on the condition that the degrees of freedom for the orthogonal array should be greater than or at least equals sum of those of wear parameters. In the present investigation, the wear parameters chosen for the experiment are (A) applied load (B) sliding velocity (C) sliding time (D) Abrasive particle size. Table 3 indicates the factors and their levels. The experiment consists of 9 tests (each row in the  $L_9$  orthogonal array) and the columns were assigned with parameters. The first column was assigned to the applied load, the second column was assigned to sliding velocity, the third column was assigned to sliding time and the fourth column was assigned to the abrasive particle size. The experimental results were transformed into a signal-to-noise (S/N) ratio. In the present study, Taguchi's the-smaller-the-better performance is measured in terms of wear rate, property which is generally expected to be as low as possible. The S/N ratio was computed for each level of process parameters using the following equation:

$$(S/N) = -10 * \log 1/n (\sum Y_i^2) \quad \dots \text{Equation (2)}$$

where  $n$  is the number of observations for one set up, and  $Y_i$  is the calculated value of wear rate for experiment number  $i$ .

**Table 2. Orthogonal array  $L_9$  ( $3^4$ ) of Taguchi**

Experiment number	A	B	C	D
1	1	1	1	1
2	1	2	2	2
3	1	3	3	3
4	2	1	2	3
5	2	2	3	1
6	2	3	1	2
7	3	1	3	2
8	3	2	1	3
9	3	3	2	1

## 7. Microstructure

The optical micrograph of the Al-Zn-Mg alloy in T6 condition at magnification 200X is shown in Figure 1. Keller's reagent (50%  $H_2O$ , 10% HF, 15% HCl and 25%  $HNO_3$ , by volume) was used as etchant. Recrystallised region, grains, grain boundary area, intermetallic particles are observed in the peak aged microstructure.

**Table 3. Process parameters with their values at three levels**

Level	Applied Load (N)	Sliding Velocity (rpm)	Sliding Time (minutes)	Abrasive Particle Size ( $\mu m$ )
	A	B	C	D
1	4.704	100	05	15.3
2	9.800	300	10	25.8
3	14.504	500	15	75.0

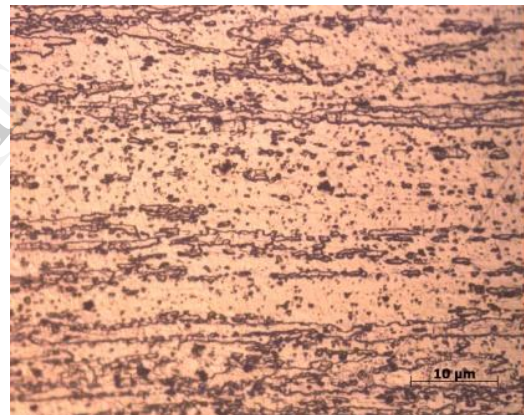


**Figure 1. Optical microstructure of the peak aged Al-Zn-Mg alloy**

## 8. Analysis of control factors

The plan of tests was developed with the aim of relating the influence of each control factor. On conducting experiments as per orthogonal array  $L_9$  ( $3^4$ ), the wear results for various combinations of parameters were obtained and are shown in Table 4. This table shows the calculated S/N ratios for each level of control factors. It can be seen from the table that the wear rate of experiment number 9 is smallest and S/N ratio is largest. The S/N response table for wear rate is presented in Table 5 using the statistical software 'MINITAB 15'. The process parameter that has the strongest influence is determined depending on the value of  $\Delta$  (delta). Delta equals the difference between the maximum and the minimum S/N ratios for a

particular process parameter. The higher the value of delta, the more influential is the control process parameter. The parameters and their interactions were sorted in relation to the values of delta. From Table 5 and Table 6, it can be seen that the strongest influence was exerted by the abrasive particle size (D).

**Table 4. Experimental design using  $L_9(3^4)$  Orthogonal array**

	A	B	C	D	Wear Rate ( $10^{-11} \text{ m}^2/\text{N}$ )	S/N Ratio
1	04.704	100	05	15.3	1.9069	-5.6066
2	04.704	300	10	25.8	2.2107	-6.8906
3	04.704	500	15	75.0	2.8716	-9.1625
4	09.800	100	10	75.0	2.7143	-8.6732
5	09.800	300	15	15.3	1.1524	-1.2321
6	09.800	500	05	25.8	1.3589	-2.6637
7	14.504	100	15	25.8	1.1988	-1.5749
8	14.504	300	05	75.0	2.6987	-8.6231
9	14.504	500	10	15.3	0.7813	2.1436

**Table 5. S/N response table for wear rate**

Level	A	B	C	D
1	-7.2199	-5.2849	-5.6311	-1.5650
2	-4.1897	-5.5819	-4.4734	-3.7097
3	-2.6848	-3.2275	-3.9898	-8.8196
$\Delta$	4.5351	2.3544	1.6413	7.2546
Rank	2	3	4	1

**Table 6. Means response table for wear rate**

Level	A	B	C	D
1	2.3297	1.9400	1.9882	3.8406
2	1.7419	2.0206	1.9021	1.5865
3	1.5596	1.6706	1.7409	2.7615
$\Delta$	0.7701	0.3500	0.2473	2.2541
Rank	2	3	4	1

The influence of controlled process parameters on wear rate are graphically represented in figures 2 and 3. Based on these response graphs, which show the variation of S/N ratio when the setting of the process parameters is changed from one level to another, the optimal combination of parameters and their levels for achieving minimum wear rate is found to be  $A_3B_3C_3D_1$  i.e. applied load at level 3 (14.504 N), sliding velocity at level 3 (500 rpm), sliding time at level 3 (15 minutes) and abrasive particle size at level 1 (15.3  $\mu\text{m}$ ). Abrasive particle size and applied load were found to be the major contributing factors for causing wear with respect to other factors. The depth of penetration increases with increasing abrasive size and decreases with increasing surface hardness of material. When abrasive particles slide on surface, it removes the material from the surface forming wear grooves. If the

size of the abrasive particles increases, the metal removal from the surface also increases [11,13,16]. Greater depth of penetration of harder SiC abrasives leads to increase in wear rate. From Table 4, the value of wear rate is greater than  $2.5 \times 10^{-11} \text{ m}^2/\text{N}$  when abrasive particle size is highest, i.e. 75 $\mu\text{m}$ . Thus wear rate increased with increasing abrasive particle size. From Table 4, for constant abrasive particle sizes, with increase in applied load, wear rate is found to decrease. This may be due to increase in contact area of the pin surface with abrasive paper with increasing load, leading to generation of heat. Due to this, formation of aluminium oxide  $\text{Al}_2\text{O}_3$  particles must have taken place which are harder than Al alloy. Thus wear resistance increased with increase in applied load and caused a decrease in wear rate.

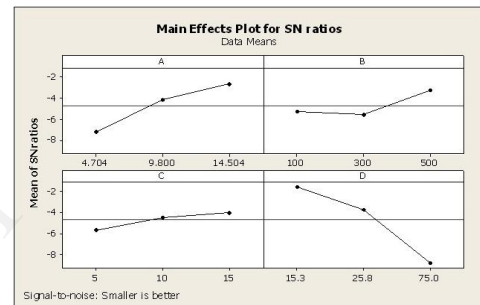


**Figure 2. Main effects plot for S/N ratios**

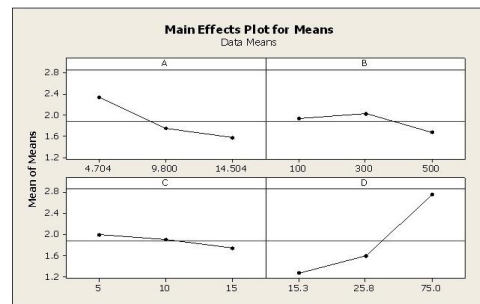


**Figure 3. Main effects plot for means**

### 8.1. Analysis of Variance (ANOVA)

Analysis of Variance was performed using statistical software 'MINITAB 15'. This analysis is carried out up to a confidence level of 95%. Table 7 shows the results of ANOVA analysis. The last column of the table indicates the percentage contribution (p) of factors on the total variation indicating the degree of their influence on the results.

From Table 7, one can easily observe that the abrasive particle size has greater influence on wear rate (p = 64.36%). Hence abrasive particle size is an important control process parameter to be taken into

account during wear. Further, applied load ( $p = 24.72\%$ ) has moderate influence, sliding velocity ( $p = 7.62\%$ ) has comparatively less influence whereas sliding time ( $p = 3.30\%$ ) has negligible influence on wear rate.

The ANOVA has resulted in zero degrees of freedom (DOF) for error term. So the factor having less influence is pooled for correct interpretation of results. Table 8 shows F-test; if  $F > 4$ , then it means that the change of design parameter has significant effect on quality characteristic. The pooled error 2% were important factors not omitted from experiments.

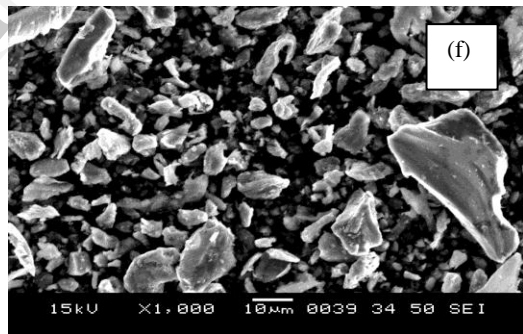
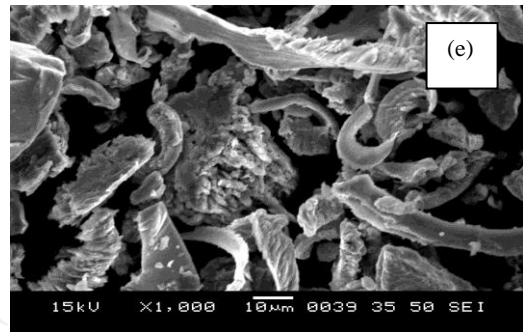
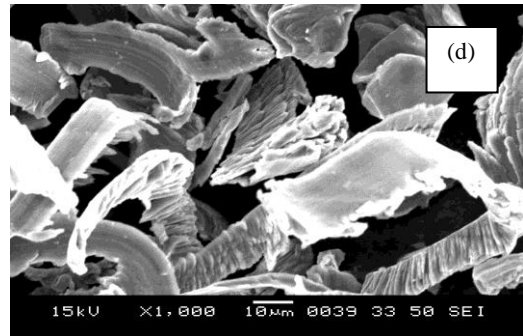
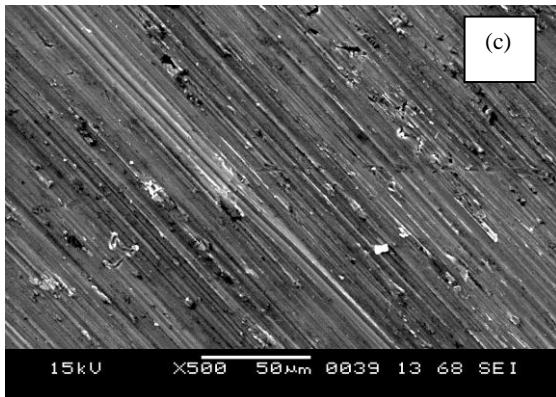
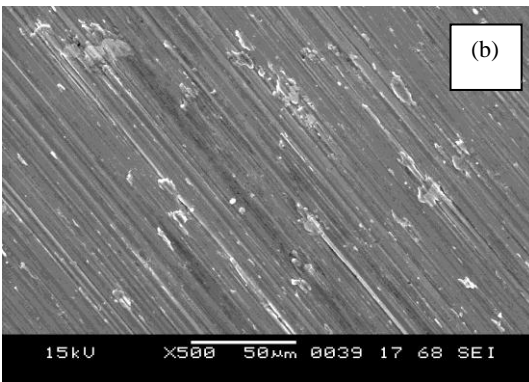
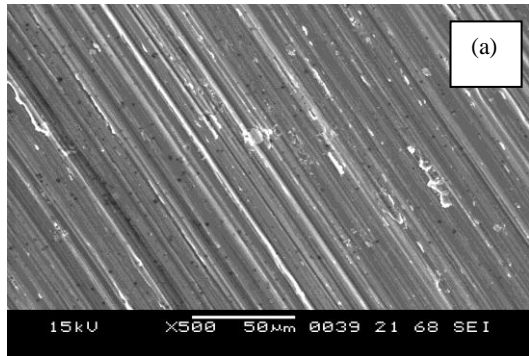


Figure 2. SEM images of wear tracks (a), (b) and (c) correspond to conditions in experiment number 3, 6 and 9 of the orthogonal array respectively. SEM images of wear debris (d), (e) and (f) correspond to conditions in experiment number 3, 6 and 9 of the orthogonal array respectively.

Table 7. Summary of ANOVA

	DOF	Sum of squares	Mean square	Percentage contribution (p%)
A	2	32.014	16.007	24.72
B	2	09.864	04.932	07.62
C	2	04.268	02.134	03.30
D	2	83.340	41.67	64.36
Error	0	-	-	
Total	8	129.486		

**Table 8. Summary of pooled ANOVA**

	DOF	Sum of squares	Mean square	F-test
A	2	32.014	16.007	07.50
B	2	09.864	04.932	02.31
D	2	83.340	41.670	19.53
Error	2	04.268	02.134	
Total	8	129.486		

**Table 9. Results of confirmation experiment**

Optimal Condition				
	Experiment	Regression model equation (3)	Difference	Error (%)
Level	A <sub>3</sub> B <sub>3</sub> C <sub>3</sub> D <sub>1</sub>	A <sub>3</sub> B <sub>3</sub> C <sub>3</sub> D <sub>1</sub>		
Wear rate (10 <sup>-11</sup> m <sup>2</sup> /N)	0.7022	0.6606	0.0416	5.92

## 8.2. Multiple linear regression model

Statistical software 'MINITAB 15' is used for developing a multiple linear regression equation. This developed model establishes a correlation between the control process parameters and the wear rate. The regression coefficient of model is 0.966. The equation obtained is as follows:

$$\text{Wear rate} = 2.14 - 0.0791 A - 0.000673 B - 0.0247 C + 0.0245 D \quad \dots \text{Equation (3)}$$

## 8.3. Confirmation Test

Once the optimal combination of process parameters and their levels was obtained, the final step was to verify the estimated results against experimental value. Confirmation test was required in the present case as the optimum combination of parameters and their levels, i.e. A<sub>3</sub>B<sub>3</sub>C<sub>3</sub>D<sub>1</sub> did not correspond to any experiment of the orthogonal array. Wear test was conducted at this optimal combination. The value of wear rate obtained from experiment was compared with the estimated value from regression model equation (3) as shown in Table 9. The difference between the experimental results and the estimated results is 0.0416. This verifies that the experimental results are strongly correlated with the estimated result, as the error is 5.92 %.

## 8.4. Wear Tracks and Debris Particles

SEM images of the wear tracks and the debris particles corresponding to experiment numbers 3, 6 and 9 of the orthogonal array are shown in figure respectively. The influence of the abrasive particle size can be noted in the figure.

It is clearly evident from wear tracks in figure 2(a) that abrasive particles of size 75 $\mu$ m (180 grit emery paper) have penetrated deeper in the material leading to formation of well defined and prominent wear scars. Debris in figure 2(d) consists of elongated flakes which are worn out from Al alloy. Wider and elongated flaky debris is a characteristic of severe wear condition [13,15,16]. Boulder materials of near-regular geometry are SiC particles worn out from abrasive paper during wear. In this case, wear rate is highest too. Wear tracks in figure 2(b), in which 400 grit emery paper, i.e., abrasive particle size of 25.8 $\mu$ m was used, indicate that the wear scars are prominent but not as deep as in figure 2(a). Debris particles in figure 2(e) comprise of a mixture of long flaky particles and near-regular shaped SiC particles contributed by Al alloy and abrasive paper respectively. This is a condition of medium wear [13,15,16]. Wear tracks in figure 2(c) indicate that the wear scars are superficial and no complete removal of the material has taken place. Debris particles in figure 2(f) are finer as the abrasive grain size was low, i.e., 15.3 $\mu$ m (600 grit emery paper). This is a case of mild wear as the wear suffered is low [13,15,16], which can also be seen from the wear rate reading in Table 4.

## 9. Conclusions

- (1) Taguchi's orthogonal design, signal-to-noise ratio (S/N), analysis of variance (ANOVA) and multiple linear regression model were successfully used for optimisation of wear parameters.
- (2) Based on the main effects plot for S/N ratios and main effects plot for means (wear rate), the optimum combination of parameters and their levels for achieving minimum wear rate is A<sub>3</sub>B<sub>3</sub>C<sub>3</sub>D<sub>1</sub>.
- (3) From the ANOVA analysis, the wear rate is dominated by different parameters in the order of abrasive particle size, having major influence (p=64.36%); followed by applied load having moderate influence (p=24.72%); sliding velocity having lesser influence (p=7.62%); and sliding time having negligible effect (p=3.30%).
- (4) Multiple linear regression model was effectively used to predict the wear rate at 95% confidence level within the range of investigation.

(5) The confirmation test showed that the error associated with dry sliding wear of the alloy with combination of optimal parameters  $A_3B_3C_3D_1$  is 5.92%.

(6) Wear rate increased with increase in abrasive particle size whereas decreased with an increase in applied load. Sliding velocity and sliding time did not affect the wear rate significantly.

## 10. References

- [1] K. Kato, "Abrasive wear of metals", *Tribology International*, 30,1997, pp.333–338.
- [2] T.S. Eyre, "Wear characteristics of metals", *Tribology International*, 10,1976, pp. 203–212.
- [3] K. Elleuch , S. Mezlini , N. Guermazi , Ph. Kapsa , "Abrasive wear of aluminium alloys rubbed against sand", *Wear*, 26(1), 2006, pp.1316–1321.
- [4] E Hatch John, *Aluminium: Properties and Physical Metallurgy*, ASM, Metals Park, Ohio, 1984.
- [5] Elwin L. Rooy, *Introduction to Aluminum and Aluminum Alloys*, ASM Handbook Vol-02.
- [6] J. R. Davis, *ASM Specialty Handbook- Aluminium and Aluminium Alloys*, ASM, April, 2002.
- [7] H Tylczak Joseph, Oregon Albany, *Abrasive Wear, Wear*, ASM handbook, Vol -18.
- [8] P. J. Ross. *Taguchi Techniques for Quality Engineering, Second Edition*, Tata McGraw-Hill Publishing Company Limited, New Delhi, 2005.
- [9] M. S. Phadke, *Quality engineering using robust design*, P. T. R. Prentice Hall Incorporation, New Jersey, 1989.
- [10] S. Gargatte, R. R. Upadhye, V. S. Dandagi, S. R. Desai, B. S. Waghmode, "Preparation and characterization of Al-5083 alloy composites", *Journal of Minerals and Materials Characterisation and Engineering*, 1,2013, pp.8-14.
- [11] Y. Sahin, "Wear behaviour of aluminium alloy and its composites reinforced by SiC particles using statistical analysis", *Materials and Design*, 24, 2003, pp.95-103.
- [12] C. Subramanian, "Some considerations towards the design of a wear resistant aluminium alloy", *Wear* 155(1), 1992, pp.193-205.
- [13] P. J. Blau, "Fifty years of research on the wear of metals", *Tribology International* 30 (5), 1997, pp. 321-331.
- [14] U. Sanchez-Santana, C. Rubio-Gonzalez, G. Gomez-Rosas, J.L. Ocana, C. Molpeceres, J. Porro, M. Morales, "Wear and friction of 6061-T6", *Wear* 260 (7-8), 2006, pp.847-854.
- [15] O. P. Modi, "Two-body abrasion of a cast Al-Cu (2014 Al) alloy- Al<sub>2</sub>O<sub>3</sub> particle composite: Influence of

heat treatment and abrasion test parameters" *Wear*, 248, 2001, pp.100-111.

[16] M. Singh, D.P. Mondal, O.P. Modi, A.K. Jha , "Two-body abrasive wear behaviour of aluminium alloy-sillimanite particle reinforced composite", *Wear* 253, 2002, pp.357–368.

[17] F. Mazzolani, *Aluminium Alloy Structures, Second edition*, E and FN Spon, an imprint of Chapman and Hall, London, UK, 1995.